

Essential Role of Extrinsic Noise in Models of *E. coli* Division Control

Mattia Corigliano^{1,2,*}, Kuheli Biswas^{4,*}, Matteo Bocchiola², Daniele

Montagnani^{2,†}, Ariel Amir^{4,‡} and Marco Cosentino Lagomarsino^{1,2,3‡}

1. IFOM-ETS, The AIRC Institute of Molecular Oncology, via Adamello 16, 20139 Milan, Italy

2. Dipartimento di Fisica, Università degli studi di Milano, via Celoria 16, 20133, Milan, Italy

3. Istituto Nazionale di Fisica Nucleare, Sezione di Milano, via Celoria 16, 20133, Milan, Italy and

4. Department of Physics of Complex Systems, Weizmann Institute of Science, Rehovot 7610001, Israel

Our understanding of cell division control in bacteria still relies largely on interpreting correlations between phenomenological variables, with limited connection to the underlying molecular mechanisms. Here, we analytically solve a stochastic threshold–accumulation model in which a size-dependent divisor protein triggers division upon reaching a noisy, autocorrelated threshold, quantifying within a unified framework the combined effects of intrinsic and extrinsic noise and key mechanistic parameters such as protein reset and threshold memory. We show that incorporating these elements yields behavior far richer than the commonly assumed *adder*, spanning a continuum of division strategies from *timer* to *sizer* while modulating size fluctuations in a nontrivial fashion. Comparison with single-cell *E. coli* data shows that extrinsic noise and additional mechanistic ingredients are required to account for the observed size fluctuations. The *adder* emerges when threshold correlations balance protein reset, generalizing the hypothesis that full reset is necessary to maintain *adder* control. Our results establish a unified analytical framework linking stochastic molecular processes to emergent division laws, to be used in more complex bacterial cell-cycle models.

Cell-cycle progression requires maintaining key physiological variables, including cell size, within specific functional ranges [1–5]. Single *E. coli* cells, for example, divide on average after adding a constant size [6, 7]. This division strategy, known as the *adder*, ensures a stable birth-size distribution with fluctuations of only 10–20% around the mean. Similar *adder*-like behavior and comparable size fluctuations have been observed across diverse organisms, including budding yeast [8–10], archaea [11], and mammalian cells [12, 13], leading to questions regarding its mechanistic origin(s).

Yet our understanding remains largely phenomenological, often relying on linearized frameworks linking fluctuations in birth size, added size, division time, and growth rate [14–17]. These analytical approaches allow us to characterize stable size distributions [16] and to test competing models of division control [18–22], but cannot explain how the observed division-control laws and size fluctuations arise from underlying molecular control processes and molecular noise sources.

To address this gap, we analyze a class of models in which a divisor molecule is synthesized at a rate proportional to cell size and triggers division upon reaching a threshold copy number [23–28]. These “threshold–accumulation” models have been proposed as minimal, biologically grounded implementations of the *adder* strategy in *E. coli* [23, 24, 26–28]

Here, we develop an analytical framework that incorporates stochastic protein accumulation (leading to in-

trinsic first-passage time noise), threshold variability (extrinsic noise), and key mechanistic ingredients such as molecule reset and threshold memory, enabling a unified treatment of intrinsic and extrinsic sources of variability. This approach bridges and extends previous studies that considered intrinsic fluctuations [29] or stochastic thresholds [30] separately, and directly links division control and size fluctuations to underlying molecular parameters.

We consider exponentially growing cells undergoing successive divisions at constant growth rate α . The empirically observed stability of the size distribution implies the presence of active division control [14]. Phenomenologically, this can be described as a coupling between fluctuations in the logarithmic birth size $q_0^{(i)} \equiv \log(s_0^{(i)}/s^*)$ and in the logarithmic added size $G^{(i)} \equiv \log(s_f^{(i)}/s_0^{(i)}) = \alpha\tau^{(i)}$, where $s_0^{(i)}$ and $s_f^{(i)}$ denote the sizes at birth and division, and $\tau^{(i)}$ the division time in cycle i . Exploiting the smallness of size fluctuations, this relation is typically linearized [14, 15] as $\delta G^{(i)} = -\lambda_G \delta q_0^{(i)} + \eta_G^{(i)}$, with $0 \leq \lambda_G \leq 1$. In this regime the logarithmic birth size follows a discrete-time Ornstein–Uhlenbeck process and the single parameter λ_G encapsulates the effective division strategy. The canonical strategies correspond to $\lambda_G = 0.5$ (*adder*: division after a constant added size), $\lambda_G = 1$ (*sizer*: division at a target size), and $\lambda_G = 0$ (*timer*: division after a fixed time). Because λ_G is directly linked to measurable statistics in single-cell data [14, 15], this framework enables inference of division strategies and tests of competing models [19]. However, it remains phenomenological and does not specify the underlying molecular dynamics.

We therefore introduce a stochastic threshold–accumulation model defined by the following ingredients. During cell cycle (i), a divisor molecule, “ x ”, is synthesized at rate, $\mu s^{(i)}$, proportional to

* These authors contributed equally to this work

† Current affiliation: Dipartimento di Matematica, Università di Pavia, Via Ferrata 5, 27100, Pavia

‡ Correspondence: ariel.amir@weizmann.ac.il, marco.cosentino-lagomarsino@ifom.eu

cell size, and division occurs when its copy number, $x^{(i)}$, first reaches a threshold $\theta^{(i)}$ [23–28] [Fig. 1]. At division, cell size is halved and the molecule is reset to $x_0^{(i+1)} = r^{(i)}\theta^{(i)}$. In what follows, we consider a constant reset, r , set either to $r = 0$ (full reset) or $r = 1/2$ (half reset), leaving the general case to the SI. Assuming deterministic exponential growth and neglecting molecular and threshold fluctuations, one has

$$s_f^{(i)} = s_0^{(i)} e^{\alpha\tau^{(i)}} = s_0^{(i)} + \frac{\alpha}{\mu}(1-r)\theta. \quad (1)$$

This simple result has led to the widespread interpretation of this model as a mechanistic realization of the *adder* [23, 28]. We show below, however, that once stochastic effects are accounted for, this correspondence holds only in restricted regions of parameter space.

Accounting for molecular noise, division timing, $\tau^{(i)}$, becomes the first-passage time of a non-homogeneous Poisson process, $\{x(t)\}$, with rate, $\mu s_0^{(i)} e^{\alpha t}$, to a fixed threshold, θ [Fig. 1(a)]. This intrinsic-noise limit was recently analyzed in a related framework in which additional degradation and constant production terms were introduced in the synthesis dynamics of the divisor protein [29]. In the absence of such terms, one has (see SI)

$$\lambda_G^{\text{intr.}} = 1/2; \quad (\text{CV}_{s_0}^2)^{\text{intr.}} = [3(1-r)\theta]^{-1}, \quad (2)$$

implying *adder* division control and Poisson scaling, $\text{CV}_{s_0} \propto 1/\sqrt{\theta}$, of size fluctuations. Reproducing the experimentally observed size variability ($\text{CV}_{s_0} \approx 10\text{--}20\%$) would then require $\theta \approx 8\text{--}70$ molecules [27]—one to two orders of magnitude smaller than realistic copy numbers of candidate division proteins, including Fts proteins such as FtsZ and FtsN [31–39], as well as peptidoglycan precursors [40–42]. Thus, within the purely size-proportional synthesis model studied here, intrinsic noise alone cannot account for the observed magnitude of size fluctuations.

One possible route to increase size variability is to introduce constant (size-independent) production (ν) or degradation (γ) terms into protein synthesis dynamics, as explored in Ref. [29]. Each term increases birth-size fluctuations and shifts division control away from the intrinsic *adder*: constant production biases toward timer-like behavior, whereas degradation promotes sizer-like regimes (see SI). Within the broader family of synthesis models parameterized by (μ, ν, γ) , the *adder* strategy was therefore identified in Ref. [29] as the one minimizing cell-size noise at fixed threshold level. While intriguing, whether such a minimization principle is biologically realized remains unclear. More importantly, our work shows that even if realized it does not uniquely support an *adder* strategy, as noise minimization preserves *adder* behavior only for a constant threshold, whereas threshold fluctuations and other mechanistic parameters shift the minimum away from the *adder* (e.g. see SI Fig. 1).

Here we follow a different route. We retain the experimentally supported size-proportional synthesis law and instead introduce additional variability at the level of

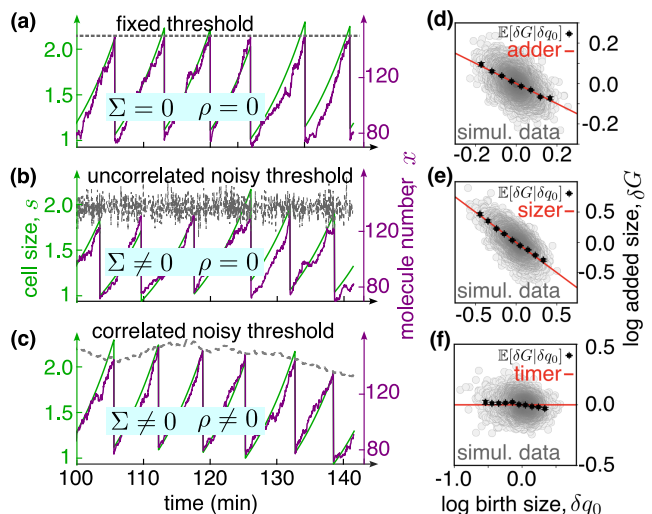


FIG. 1. Model dynamics and threshold regimes. Exponentially growing single cells undergoing successive divisions. Division occurs when a divisor molecule $x(t)$, produced proportionally to cell size $s(t)$, reaches a threshold that is either (a) constant or (b,c) fluctuating, with uncorrelated or autocorrelated dynamics and memory ρ . The noise ratio is $\Sigma = \text{CV}_{\text{th}}/\text{CV}_{\text{mol}}$, with $\Sigma = 0$ in (a) and $\Sigma > 0$ in (b,c).

the division threshold [Fig. 1(b–c)]. Despite its minimal structure, the model remains analytically tractable and, as we show below, rich enough to generate diverse behaviors [Fig. 1(d–f)].

Specifically, we consider fluctuations in the threshold level, $\xi^{(i)} \equiv \theta^{(i)} - \mathbb{E}[\theta]$, as a primary source of extrinsic noise. Such fluctuations may reflect variability in the molecular components setting the division trigger or, more generally, an effective activated process with a fluctuating barrier height [43, 44]. We model the discrete-time dynamics of threshold fluctuations as

$$\xi^{(i)} = \rho \xi^{(i-1)} + \eta^{(i)}, \quad \text{with } \eta^{(i)} \stackrel{\text{i.i.d.}}{\sim} \mathcal{N}(0, \sigma_{\text{extr}}^2) \quad (3)$$

where σ_{extr}^2 represents extrinsic noise and ρ quantifies memory between successive cycles [Fig. 1(b)–(c)]. Threshold (and size) fluctuations are stable for $|\rho| < 1$, with $\text{Var}[\theta] = \sigma_{\text{extr}}^2/(1 - \rho^2)$ and $\text{Cov}[\theta^{(i)}, \theta^{(i-k)}] = \rho^k \text{Var}[\theta]$. In what follows, we restrict to $\rho \in (0, 1)$ for the half-reset case ($r = \frac{1}{2}$), and $\rho \in (-\frac{1}{2}, 1)$ for the full-reset case ($r = 0$), yielding the standard monotonic size-control regime with $\lambda_G \in (0, 1)$ (see below). For $\rho > 0$, Eq. (3) reduces to a discretely sampled Ornstein–Uhlenbeck process with correlation time $\tau_\xi = -\tau/\log \rho$, recovering previously studied models [30].

Crucially, threshold fluctuations make the first-passage time in cycle (i) depend on the molecular increment required for division, $\Delta x^{(i)}$, whose fluctuations obey

$$\Delta x^{(i)} - (1-r)\mathbb{E}[\theta] = (\rho-r)\xi^{(i-1)} + \eta^{(i)}. \quad (4)$$

To compute the division-control parameter and size fluctuations in this regime, we can therefore use the expres-

sions $\lambda_G = -\alpha \mathbb{E}[s_0] \frac{d\mathbb{E}[\tau^{(i)}|s_0^{(i)}]}{ds_0^{(i)}} \Big|_{\mathbb{E}[s_0]} = 1 - \frac{1}{2} \frac{\text{Cov}[s_f, s_0]}{\text{Var}[s_0]}$, and $\text{CV}_{s_0}^2 = \frac{\alpha^2 \mathbb{E}[\text{Var}[\tau^{(i)}|s_0^{(i)}]]}{\lambda_G(2-\lambda_G)}$, upon applying the laws of total expectation and variance to $\mathbb{E}[\tau^{(i)}|s_0^{(i)}, \Delta x^{(i)}]$ and $\text{Var}[\tau^{(i)}|s_0^{(i)}, \Delta x^{(i)}]$. Remarkably, both quantities can be written as their intrinsic limits (Eq. (2)), multiplied by a modulation depending on two dimensionless parameters: (i) the threshold autocorrelation ρ , and (ii) the relative strength of extrinsic to molecular noise, $\Sigma \equiv \text{CV}_{\text{extr.}}^2 / \text{CV}_{\text{mol.}}^2$, where $\text{CV}_{\text{extr.}}^2 = \sigma_{\text{extr.}}^2 / \mathbb{E}[\theta]^2$ and $\text{CV}_{\text{mol.}}^2 = [(1-r)\mathbb{E}[\theta]]^{-1}$. The resulting expressions take the compact form (see SI for analytical derivations)

$$\begin{aligned} \frac{\lambda_G(\Sigma, \rho)}{\lambda_G^{\text{intr.}}} &= 1 - \frac{1}{2} \frac{(\rho-r)(1-r\rho)}{(1-r)^2(1-\rho/2)} \frac{\text{CV}_\theta^2}{\text{CV}_{s_0}^2}(\Sigma, \rho), \\ \frac{\text{CV}_{s_0}^2(\Sigma, \rho)}{(\text{CV}_{s_0}^2)^{\text{intr.}}} &= 1 + \frac{(1+r^2)(1+\frac{\rho}{2}) - r(1+2\rho)}{(1-r)^2(1-\rho/2)(1-\rho^2)} \Sigma^2, \end{aligned} \quad (5)$$

with $\text{CV}_\theta^2(\Sigma, \rho) = \frac{3(\text{CV}_{s_0}^2)^{\text{intr.}} \Sigma^2}{1-\rho^2}$. The full dependence of the division strategy (λ_G) and birth-size fluctuations ($\text{CV}_{s_0}^2$) on threshold memory ρ , noise strength Σ , and reset fraction r is summarized in Fig. 2. Contrary to the common view that such models generically implement a simple *adder*, we find that they realize a broad and continuously tunable range of behaviors. In particular, the model captures the full spectrum of division strategies, from *sizer* to *timer*, while allowing size fluctuations to vary from negligible to experimentally relevant levels.

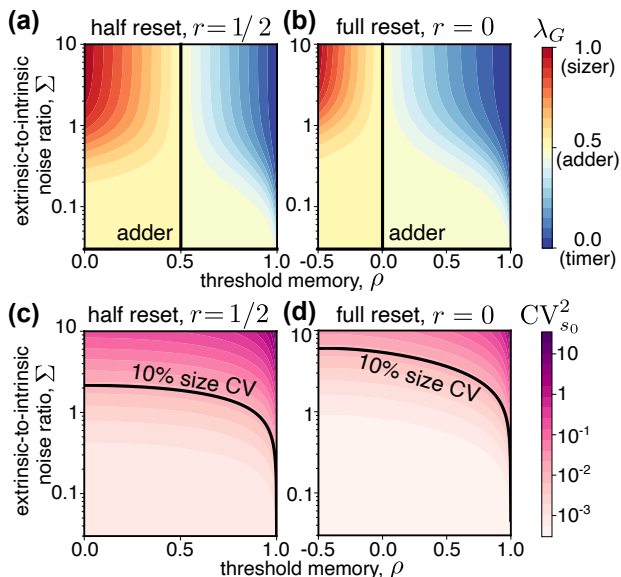


FIG. 2. **Model predictions.** Contour plots of the division-control parameter λ_G (a,b) and birth-size fluctuations $\text{CV}_{s_0}^2$ (c,d) from Eq. (5) with a plausible value of $\theta = 1000$ [31–42], for $r = 1/2$ (a,c) and $r = 0$ (b,d).

As expected, in the intrinsic-noise limit ($\Sigma \rightarrow 0$), the model recovers *adder* behavior [29], which, however, is associated with unrealistically small size fluctuations at

typical protein copy numbers. In addition to this known limit, we uncover a qualitatively distinct *adder* regime in which division control remains *adder* while size fluctuations are independently tunable. This occurs when threshold memory matches the reset fraction ($\rho = r$), defining a “memory-balance” [Fig. 2(a–b)], where $\lambda_G = 1/2$ and $\text{CV}_{s_0}^2 \rightarrow \frac{1}{3(1-r)(\theta)} \left(1 + \frac{\Sigma^2}{1-r}\right)$. In this regime, size variability increases continuously with threshold noise without affecting division control [Fig. 2(c–d)], thereby decoupling size fluctuations from the underlying control strategy. This decoupling originates from a cancellation of memory effects (Eq. (4)): when $\rho = r$, correlations in the threshold exactly compensate the memory introduced by protein inheritance at division, rendering the accumulated increment statistically independent across cycles and thereby restoring *adder* control. Thus, *adder* behavior does not require full protein reset. Instead, full reset ($r = 0$) yields *adder* control only when threshold fluctuations are uncorrelated ($\rho = 0$), whereas in general the condition is $\rho = r$. This revises the standard intuition that full protein reset is necessary for *adder* control in presence of threshold noise. We note that this behavior contrasts with models such as Ref. [29], in which increasing size fluctuations via degradation or constant production terms simultaneously alters the division strategy, and that in those models degradation can be seen as a contributor to memory-balance.

Away from the $\rho = r$ line, increasing threshold noise drives the system away from the intrinsic *adder* limit ($\Sigma \rightarrow 0$), shifting division control toward either sizer-like ($\rho < r$) or timer-like behavior ($\rho > r$) [Fig. 2(a)]. Access to both regimes requires partial inheritance of the divisor molecule ($r > 0$). In the fully reset case ($r = 0$), division control is instead confined to interpolate between *adder* and *timer*, except when negatively correlated fluctuations are allowed ($\rho < 0$), which enable recovery of sizer-like behavior [Fig. 2(b)]. Specifically, in the large-noise limit ($\Sigma \gg 1$), the asymptotic behavior reads $\frac{\text{CV}_{s_0}^2}{\text{CV}_\theta^2} \rightarrow \frac{(1+r^2)(1+\rho/2)-r(1+2\rho)}{3(1-r)^2(1-\rho/2)}$ and $\lambda_G \rightarrow \frac{1}{2} \left\{ 1 + \frac{3}{2} \frac{(\rho-r)(\rho r-1)}{(1+r^2)(1+\rho/2)-r(1+2\rho)} \right\}$. For $r = \frac{1}{2}$, one obtains $\text{CV}_{s_0}^2 \rightarrow \text{CV}_\theta^2$ independently of ρ and $\lambda_G \rightarrow 1 - \rho$, so that division control spans the full range from perfect *sizer* ($\rho = 0$) to perfect *timer* ($\rho = 1$). By comparison, for $r = 0$, $\text{CV}_{s_0}^2 \rightarrow \frac{2+\rho}{3(2-\rho)} \text{CV}_\theta^2$ and $\lambda_G \rightarrow \frac{1}{2} \left(1 - \frac{3\rho}{2+\rho}\right)$, yielding a continuous interpolation from perfect *sizer* at $\rho = -1/2$ to perfect *timer* at $\rho = 1$.

In the fully autocorrelated limit ($\rho \rightarrow 1$), the model approaches a perfect *timer*, with $\text{CV}_{s_0}^2 \rightarrow \text{CV}_\theta^2$ and $\lambda_G \rightarrow 0$, independently of Σ and r , provided $\Sigma \neq 0$. This may appear paradoxical, since in this limit $\theta^{(i)} \simeq \theta^{(i-1)} + \eta^{(i)}$, implying that over finite timescales its deviations from the initial value remain small with high probability, especially when extrinsic noise is weak. More precisely, for any finite extrinsic noise, there exists a characteristic number of generations \mathcal{L} over which the threshold remains within a fraction ϵ of its initial value θ^0 with con-

confidence p : $\mathcal{L} \approx \left(\frac{\epsilon \theta^0}{z_{(1+p)/2} \sigma_{\text{extr.}}} \right)^2$. Over such timescales, the threshold is effectively constant, which would suggest adder-like behavior. The resolution lies in variability across lineages. Individual lineages behave approximately as *adders* for $\lesssim \mathcal{L}$ generations, but differences in the inherited threshold θ^0 dominate at longer times and give rise to an emergent *timer* at the population level (SI Fig. 2). This instance of Simpson’s paradox highlights a nontrivial interplay between lineage and population behavior.

Finally, to compare the model predictions with available *E. coli* single-cell data, we focused on the predicted relationship between size fluctuations, $\text{CV}^2(s_0)$, and the division-control parameter, λ_G , and sourced measurements from seven independent studies [7, 20, 26, 45–48]. Consistent with previous analyses, the data cluster near the *adder* regime ($\lambda_G \simeq 0.5$), with a weak shift toward sizer-like behavior at low growth rates, and exhibit birth-size fluctuations in the range $\text{CV}^2(s_0) \sim 10^{-2} - 4 \times 10^{-2}$ [Fig. 3]. Comparing these trends with

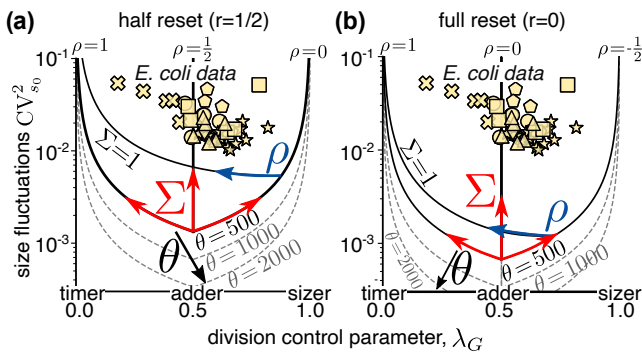


FIG. 3. Extrinsic sources of noise are needed to fit *E. coli* data at realistic divisor molecule numbers. (a–b) Predicted joint modulation of birth-size fluctuations ($\text{CV}^2(s_0)$) and division control (λ_G) as model parameters (Σ, ρ, θ) vary, for partial reset ($r = 1/2$, a) and full reset ($r = 0$, b). (c) Single-cell measurements from seven independent microfluidic experiments on *E. coli* cluster near the *adder* regime ($\lambda_G \simeq 0.5$) with birth-size fluctuations of ~ 10 –20%.

the full range of model predictions obtained by varying (ρ, Σ, r, θ) [Fig. 3(a),(b)], we first observe that decreasing the threshold level shifts the entire manifold upward by increasing the intrinsic baseline of size fluctuations. At biologically realistic molecule numbers ($\sim 10^3$ [31–42]), the model nevertheless cannot access the experimental region without extrinsic noise, indicating that extrinsic noise is essential to reproduce the observed size statistics.

In the presence of extrinsic noise, agreement with the data is achieved in a memory-balanced *adder* regime, $\rho \approx r$. In this regime, threshold fluctuations modulate size variability while maintaining division control close to the observed adder. When the memory-balanced condition is perturbed, $\rho > r$ promotes timer-like behavior and $\rho < r$ promotes sizer-like behavior. (The well-studied scenario of full resetting is a particular case of this class

of models, for which $\rho = r = 0$.) Additional biological ingredients not included in our main framework, such as active protein degradation or constant production, also tune division control and size fluctuations (SI Fig. 1), extending the accessible regimes [29].

In this work, we investigated the role of extrinsic noise in a stochastic threshold–accumulation model for cell division. Contrary to common assumptions [26, 28, 29], we uncover a phenomenology that extends beyond simple *adder* behavior. By solving the model analytically, we derived explicit relationships linking division control to size fluctuations, connecting underlying stochastic molecular processes to emergent phenomenological laws. We should note that although stochastic accumulation rules with threshold variability and memory already capture a rich phenomenology, chromosome replication and segregation are also known to play central roles in *E. coli* cell-division control [18–21, 49].

While incorporating threshold-accumulation processes into a more complete theory remains an important challenge, our analysis leads to three key results. First, intrinsic stochasticity alone, although it naturally generates *adder*-like correlations, predicts size fluctuations that are significantly smaller than those observed in *E. coli* for realistic threshold molecule numbers [31–42]. A systematic exploration of the model shows that extrinsic variability—specifically, fluctuations in the division threshold—is an essential ingredient for quantitatively capturing experimental observations within a threshold-accumulation framework.

Second, we connect the size-control parameter to the amplitude and memory of the extrinsic noise. *Adder* behavior emerges when threshold memory compensates for molecular reset at division, i.e., the retained fraction of the divisor protein, independent of noise amplitude.

Finally, our results show that the *adder* principle does not, in general, minimize size variability in the presence of extrinsic noise, as the optimal control strategy becomes explicitly noise-dependent. In this setting, constrained optimization does not provide a well-defined route to an optimality principle, since relative fluctuations can always be reduced by tuning the threshold. Even in the absence of extrinsic noise, optimization over a restricted set of parameters (e.g., the degradation rate alone) lacks a clear biological basis, as evolutionary processes can act on multiple control variables. Taken together, these findings challenge the view that *adder* correlations arise from variability minimization and instead point to a broader, noise-dependent landscape of size-control strategies. Whether minimizing size variability is itself under selection remains unclear [50–53], leaving the origin of the widely observed *adder* correlations an open question.

We thank Gabriele Micali for useful discussions. This work was supported by Fondazione AIRC per la ricerca sul cancro ETS (AIRC IG 2019 Grant No. 23258 and AIRC IG 2024 Grant No. 30391—P.I. M. C. L.). M.C. was supported by Fondazione AIRC per la ricerca sul

cancro ETS (ID. 28177). A.A. and K.B. were supported

by the European Union (ERC, BIGR, 101125981) and Israeli Science Foundation (146873).

-
- [1] M. B. Ginzberg, R. Kafri, and M. Kirschner, Cell biology. on being the right (cell) size, *Science* **348**, 1245075 (2015).
- [2] G. E. Neurohr, R. L. Terry, J. Lengefeld, M. Bonney, G. P. Brittingham, F. Moretto, T. P. Miettinen, L. P. Vaites, L. M. Soares, J. A. Paulo, J. W. Harper, S. Buratowski, S. Manalis, F. J. van Werven, L. J. Holt, and A. Amon, Excessive cell growth causes cytoplasm dilution and contributes to senescence, *Cell* **176**, 1083 (2019).
- [3] G. E. Neurohr and A. Amon, Relevance and regulation of cell density, *Trends Cell Biol.* **30**, 213 (2020).
- [4] S. Xie, M. Swaffer, and J. M. Skotheim, Eukaryotic cell size control and its relation to biosynthesis and senescence, *Annu. Rev. Cell Dev. Biol.* **38**, 291 (2022).
- [5] J. Lengefeld and E. Zatulovskiy, Editorial: Cell size regulation: molecular mechanisms and physiological importance, *Front. Cell Dev. Biol.* **11**, 1219294 (2023).
- [6] M. Campos, I. V. Surovtsev, S. Kato, A. Paintdakhi, B. Beltran, S. E. Ebmeier, and C. Jacobs-Wagner, A constant size extension drives bacterial cell size homeostasis, *Cell* **159**, 1433 (2014).
- [7] S. Taheri-Araghi, S. Bradde, J. T. Sauls, N. S. Hill, P. A. Levin, J. Paulsson, M. Vergassola, and S. Jun, Cell-size control and homeostasis in bacteria, *Curr. Biol.* **25**, 385 (2015).
- [8] I. Soifer, L. Robert, and A. Amir, Single-cell analysis of growth in budding yeast and bacteria reveals a common size regulation strategy, *Curr. Biol.* **26**, 356 (2016).
- [9] D. Chandler-Brown, K. M. Schmoller, Y. Winetraub, and J. M. Skotheim, The adder phenomenon emerges from independent control of pre- and post-start phases of the budding yeast cell cycle, *Curr. Biol.* **27**, 2774 (2017).
- [10] C. Garmendia-Torres, O. Tassy, A. Matifas, N. Molina, and G. Charvin, Multiple inputs ensure yeast cell size homeostasis during cell cycle progression, *eLife* **7**, e34025 (2018).
- [11] Y. J. Eun, P. Y. Ho, M. Kim, S. LaRussa, L. Robert, L. D. Renner, A. Schmid, E. Garner, and A. Amir, Archaeal cells share common size control with bacteria despite noisier growth and division, *Nat. Microbiol.* **3**, 148 (2017).
- [12] C. Cadart, S. Monnier, J. Grilli, P. J. Sáez, N. Srivastava, R. Attia, E. Terriac, B. Baum, M. Cosentino-Lagomarsino, and M. Piel, Size control in mammalian cells involves modulation of both growth rate and cell cycle duration, *Nat. Commun.* **9**, 3275 (2018).
- [13] E. Levien, J. H. Kang, K. Biswas, S. R. Manalis, A. Amir, and T. P. Miettinen, Stochasticity in mammalian cell growth rates drives cell-to-cell variability independently of cell size and divisions, *Proc. Natl. Acad. Sci. U. S. A.* **123**, e2516372123 (2026).
- [14] A. Amir, Cell size regulation in bacteria, *Phys. Rev. Lett.* **112** (2014).
- [15] J. Grilli, M. Osella, A. S. Kennard, and M. C. Lagomarsino, Relevant parameters in models of cell division control, *Phys. Rev. E.* **95** (2017).
- [16] P. Y. Ho, J. Lin, and A. Amir, Modeling cell size regulation: From single-cell-level statistics to molecular mechanisms and population-level effects, *Annu. Rev. Biophys.* **47**, 251 (2018).
- [17] J. Grilli, C. Cadart, G. Micali, M. Osella, and M. Cosentino Lagomarsino, The empirical fluctuation pattern of e. coli division control, *Front. Microbiol.* **9** (2018).
- [18] G. Micali, J. Grilli, M. Osella, and M. Cosentino Lagomarsino, Concurrent processes set e. coli cell division, *Sci. Adv.* **4**, eaau3324 (2018).
- [19] G. Micali, J. Grilli, J. Marchi, M. Osella, and M. Cosentino Lagomarsino, Dissecting the control mechanisms for DNA replication and cell division in e. coli, *Cell Rep.* **25**, 761 (2018).
- [20] A. Colin, G. Micali, L. Faure, M. Cosentino Lagomarsino, and S. van Teeffelen, Two different cell-cycle processes determine the timing of cell division in *Escherichia coli*, *eLife* **10**, e67495 (2021).
- [21] S. Tiruvadi-Krishnan, J. Männik, P. Kar, J. Lin, A. Amir, and J. Männik, Coupling between DNA replication, segregation, and the onset of constriction in *Escherichia coli*, *Cell Rep.* **38**, 110539 (2022).
- [22] P. Kar, S. Tiruvadi-Krishnan, J. Männik, J. Männik, and A. Amir, Using conditional independence tests to elucidate causal links in cell cycle regulation in *Escherichia coli*, *Proc. Natl. Acad. Sci. U. S. A.* **120**, e2214796120 (2023).
- [23] L. K. Harris and J. A. Theriot, Relative rates of surface and volume synthesis set bacterial cell size, *Cell* **165**, 1479 (2016).
- [24] F. Barber, P. Y. Ho, A. W. Murray, and A. Amir, Details matter: Noise and model structure set the relationship between cell size and cell cycle timing, *Front. Cell Dev. Biol.* **5** (2017).
- [25] N. Ojkic, D. Serbanescu, and S. Banerjee, Surface-to-volume scaling and aspect ratio preservation in rod-shaped bacteria, *eLife* **8**, e47033 (2019).
- [26] F. Si, G. Le Treut, J. T. Sauls, S. Vadia, P. A. Levin, and S. Jun, Mechanistic origin of cell-size control and homeostasis in bacteria, *Curr. Biol.* **29**, 1760 (2019).
- [27] P. P. Pandey, H. Singh, and S. Jain, Exponential trajectories, cell size fluctuations, and the adder property in bacteria follow from simple chemical dynamics and division control, *Phys. Rev. E.* **101**, 062406 (2020).
- [28] M. Panlilio, J. Grilli, G. Tallarico, I. Iuliani, B. Scavi, P. Cicuta, and M. Cosentino Lagomarsino, Threshold accumulation of a constitutive protein explains e. coli cell-division behavior in nutrient upshifts, *Proc. Natl. Acad. Sci. U. S. A.* **118** (2021).
- [29] M. ElGamal and A. Mugler, Effects of molecular noise on cell size control, *Phys. Rev. Lett.* **132**, 098403 (2024).
- [30] L. Luo, Y. Bai, and X. Fu, Stochastic threshold in cell size control, *Phys. Rev. Res.* **5** (2023).
- [31] J. Pla, M. Sánchez, P. Palacios, M. Vicente, and M. Aldea, Preferential cytoplasmic location of FtsZ, a protein essential for *Escherichia coli* septation, *Mol. Microbiol.* **5**, 1681 (1991).

- [32] S. Rueda, M. Vicente, and J. Mingorance, Concentration and assembly of the division ring proteins FtsZ, FtsA, and ZipA during the escherichia coli cell cycle, *J. Bacteriol.* **185**, 3344 (2003).
- [33] A. Ursinus, F. van den Ent, S. Brechtel, M. de Pedro, J.-V. Höltje, J. Löwe, and W. Vollmer, Murein (peptidoglycan) binding property of the essential cell division protein FtsN from escherichia coli, *J. Bacteriol.* **186**, 6728 (2004).
- [34] T. Mohammadi, G. E. J. Ploeger, J. Verheul, A. D. Comvalius, A. Martos, C. Alfonso, J. van Marle, G. Rivas, and T. den Blaauwen, The GTPase activity of escherichia coli FtsZ determines the magnitude of the FtsZ polymer bundling by ZapA in vitro, *Biochemistry* **48**, 11056 (2009).
- [35] H. P. Erickson, D. E. Anderson, and M. Osawa, FtsZ in bacterial cytokinesis: cytoskeleton and force generator all in one, *Microbiol. Mol. Biol. Rev.* **74**, 504 (2010).
- [36] G. W. Li, D. Burkhardt, C. Gross, and J. S. Weissman, Quantifying absolute protein synthesis rates reveals principles underlying allocation of cellular resources, *Cell* **157**, 624 (2014).
- [37] B. Liu, L. Persons, L. Lee, and P. A. J. de Boer, Roles for both FtsA and the FtsBLQ subcomplex in FtsN-stimulated cell constriction in escherichia coli, *Mol. Microbiol.* **95**, 945 (2015).
- [38] N. O. E. Vischer, J. Verheul, M. Postma, B. van den Berg van Saparoea, E. Galli, P. Natale, K. Gerdes, J. Luirink, W. Vollmer, M. Vicente, and T. den Blaauwen, Cell age dependent concentration of escherichia coli divisome proteins analyzed with ImageJ and ObjectJ, *Front. Microbiol.* **6**, 586 (2015).
- [39] A. J. F. Egan and W. Vollmer, The stoichiometric divisome: a hypothesis, *Front. Microbiol.* **6**, 455 (2015).
- [40] W. D. Ramey and E. E. Ishiguro, Site of inhibition of peptidoglycan biosynthesis during the stringent response in escherichia coli, *J. Bacteriol.* **135**, 71 (1978).
- [41] Y. van Heijenoort, M. Gómez, M. Derrien, J. Ayala, and J. van Heijenoort, Membrane intermediates in the peptidoglycan metabolism of escherichia coli: possible roles of PBP 1b and PBP 3, *J. Bacteriol.* **174**, 3549 (1992).
- [42] J. van Heijenoort, Lipid intermediates in the biosynthesis of bacterial peptidoglycan, *Microbiol. Mol. Biol. Rev.* **71**, 620 (2007).
- [43] N. G. Van Kampen, *Stochastic processes in physics and chemistry*, 3rd ed., North-Holland Personal Library (North-Holland, Oxford, England, 2007).
- [44] C. Gardiner, *Stochastic Methods. A Handbook for the Natural and Social Sciences*, 5th ed., Springer Series in Synergetics (Springer Berlin Heidelberg, 2009).
- [45] A. Adiciptaningrum, M. Osella, M. C. Moolman, M. Cosentino Lagomarsino, and S. J. Tans, Stochasticity and homeostasis in the e. coli replication and division cycle, *Sci. Rep.* **5**, 18261 (2015).
- [46] A. S. Kennard, M. Osella, A. Javer, J. Grilli, P. Nghe, S. J. Tans, P. Cicuta, and M. Cosentino Lagomarsino, Individuality and universality in the growth-division laws of single e. coli cells, *Phys. Rev. E.* **93**, 012408 (2016).
- [47] M. Wallden, D. Fange, E. G. Lundius, Ö. Baltekin, and J. Elf, The synchronization of replication and division cycles in individual e. coli cells, *Cell* **166**, 729 (2016).
- [48] G. Witz, E. van Nimwegen, and T. Julou, Initiation of chromosome replication controls both division and replication cycles in *E. coli* through a double-adder mechanism, *eLife* **8**, e48063 (2019).
- [49] P. Y. Ho and A. Amir, Simultaneous regulation of cell size and chromosome replication in bacteria, *Front. Microbiol.* **6**, 662 (2015).
- [50] J. Lin and A. Amir, The effects of stochasticity at the single-cell level and cell size control on the population growth, *Cell Systems* **5**, 358 (2017).
- [51] E. Levien, J. Min, J. Kondev, and A. Amir, Non-genetic variability in microbial populations: survival strategy or nuisance?, *Reports on Progress in Physics* **84**, 116601 (2021).
- [52] S. Hobson-Gutierrez and E. Kussell, Evolutionary advantage of cell size control, *Phys. Rev. Lett.* **134**, 118401 (2025).
- [53] F. Proulx-Giraldeau, J. M. Skotheim, and P. François, Evolution of cell size control is canalized towards adders or sizers by cell cycle structure and selective pressures, *eLife* **11**, e79919 (2022).

Supplementary Information for “Essential Role of Extrinsic Noise in Models of *E. coli* Division Control”

A. PHENOMENOLOGICAL FRAMEWORK FOR CELL DIVISION CONTROL

We begin by briefly reviewing key concepts and quantities in the phenomenological study of division control [1–3].

At the phenomenological level, division control in exponentially growing cells is described by a control function $\delta G^{(i)}(\delta q_0^{(i)})$, linking fluctuations in the added logarithmic size $G^{(i)} \equiv \log(s_f^{(i)}/s_0^{(i)})$ to those in the logarithmic birth size $q_0^{(i)} \equiv \log(s_0^{(i)}/s^*)$ at cell cycle (i) [1].

Motivated by the smallness of fluctuations around the mean, the control function is commonly linearized [1–3] as $\delta G^{(i)} \approx -\lambda_G \delta q_0^{(i)} + \eta_G^{(i)}$, where

$$\lambda_G \equiv -\left. \frac{d\mathbb{E}[G^{(i)}|q_0^{(i)}]}{dq_0^{(i)}} \right|_{q_0^{(i)}=\mathbb{E}[q_0]}. \quad (\text{S1})$$

Importantly, the division control parameter λ_G introduced by this linear approximation can be directly estimated from the data as

$$\lambda_G = -\frac{\text{Cov}[G^{(i)}, q_0^{(i)}]}{\text{Var}[q_0]}, \quad (\text{S2})$$

and used to distinguish between different division control strategies. Alternatively, one may consider the control function $\delta \Delta s^{(i)}(\delta s_0^{(i)})$, defined in terms of the added size $\Delta s^{(i)} \equiv s_f^{(i)} - s_0^{(i)}$, with the corresponding control parameter

$$\zeta_\Delta \equiv -\left. \frac{d\mathbb{E}[\Delta s^{(i)}|s_0^{(i)}]}{ds_0^{(i)}} \right|_{s_0^{(i)}=\mathbb{E}[s_0]} = -\frac{\text{Cov}[\Delta s^{(i)}, s_0^{(i)}]}{\text{Var}[s_0]}. \quad (\text{S3})$$

The two formulations are equivalent to first order, describing the same underlying control mechanism in different variables, and are related by [4]

$$\lambda_G = 1 - \frac{\mathbb{E}[s_0]}{\mathbb{E}[s_f]}(1 - \zeta_\Delta) = 1 - \frac{1}{2}(1 - \zeta_\Delta), \quad (\text{S4})$$

where the last equality holds for symmetric division. For an adder, cells add on average a constant, size-independent increment $s_f^{(i)} = s_0^{(i)} + \Delta + \text{noise}$, hence $\zeta_\Delta = 0$ and $\lambda_G = 1 - \mathbb{E}[s_0]/\mathbb{E}[s_f]$. Furthermore, if division is symmetric, $\lambda_G = \frac{1}{2}$ for an adder.

Within this framework, the logarithmic birth size follows a discrete-time first order autoregressive process

$$\delta q_0^{(i)} = (1 - \lambda_G)\delta q_0^{(i-1)} + \eta^{(i-1)}, \quad (\text{S5})$$

converging to a stationary distribution for $0 < \lambda_G < 2$ (equivalently, $1 - \frac{\mathbb{E}[s_f]}{\mathbb{E}[s_0]} < \zeta_\Delta < 1 + \frac{\mathbb{E}[s_f]}{\mathbb{E}[s_0]}$) [1, 2]. In this limit, birth-size fluctuations satisfy

$$\text{CV}_{s_0} = \sqrt{\frac{\text{Var}[\eta_G]}{\lambda_G(2 - \lambda_G)}} = \sqrt{\frac{\mathbb{E}[\text{Var}[G^{(i)}|q_0^{(i)}]]}{\lambda_G(2 - \lambda_G)}}, \quad (\text{S6})$$

and are (apparently! [5]) minimized by a ‘‘sizer’’ ($\lambda_G = \zeta_\Delta = 1$).

B. DIVISION CONTROL IN PRESENCE OF MOLECULAR NOISE

Considering molecular noise on the accumulation of the divisor molecule ‘‘x’’, synthesized at a rate $\mu s_0 e^{\alpha t}$, division time becomes the first passage time of a non-homogenous Poisson process (NHPP), $x(t)$, to a fixed threshold θ , starting from an initial amount $r\theta$:

$$\tau^{(i)} = \inf\{t > 0 : x^{(i)}(t) - x_0 \geq (1 - r)\theta\}. \quad (\text{S7})$$

The first passage time statistics are related to the division control parameter, λ_G , and the birth size fluctuations, $\text{CV}_{s_0}^2$, through Eq. (S1) and Eq. (S6), respectively, and the relation $G^{(i)} = \alpha^{(i)}\tau^{(i)}$, valid under exponential growth. Assuming a constant growth rate, α , we have

$$\lambda_G = -\alpha \mathbb{E}[s_0] \frac{d\mathbb{E}[\tau^{(i)}|s_0^{(i)}]}{ds_0^{(i)}} \Big|_{\mathbb{E}[s_0]}, \quad \text{CV}_{s_0}^2 = \frac{\alpha^2 \mathbb{E}[\text{Var}[\tau^{(i)}|s_0^{(i)}]]}{\lambda_G(2 - \lambda_G)}. \quad (\text{S8})$$

The conditional expectation and variance of the FPT of a NHPP can be written as [6, 7]

$$\mathbb{E}[\tau^{(i)}|s_0^{(i)}] = \frac{1}{\alpha} \mathbb{E} \left[\log \left(1 + \frac{\alpha}{\mu s_0^{(i)}} Y \right) \right]; \quad \text{Var}[\tau^{(i)}|s_0^{(i)}] = \frac{1}{\alpha^2} \text{Var} \left[\log \left(1 + \frac{\alpha}{\mu s_0^{(i)}} Y \right) \right], \quad (\text{S9})$$

with $Y \sim \text{Gamma}((1 - r)\theta, 1)$. For large threshold values, $\theta \gg 1$, we can exploit the normal approximation, $Y \approx (1 - r)\theta + \sqrt{(1 - r)\theta} Z$, with $Z \sim \mathcal{N}(0, 1)$, to write

$$\log \left(1 + \frac{\alpha}{\mu s_0^{(i)}} Y \right) \approx \log \left(1 + \frac{\alpha}{\mu s_0^{(i)}} (1 - r)\theta \right) + \frac{\frac{\alpha}{\mu s_0^{(i)}} \sqrt{(1 - r)\theta}}{1 + \frac{\alpha}{\mu s_0^{(i)}} (1 - r)\theta} Z. \quad (\text{S10})$$

Therefore,

$$\mathbb{E}[\tau^{(i)}|s_0^{(i)}] = \frac{1}{\alpha} \log \left(1 + \frac{\alpha}{\mu s_0^{(i)}} (1-r)\theta \right); \quad \text{Var}[\tau^{(i)}|s_0^{(i)}] = \frac{1}{\alpha^2} \frac{\left(\frac{\alpha}{\mu s_0^{(i)}} \right)^2 (1-r)\theta}{\left(1 + \frac{\alpha}{\mu s_0^{(i)}} (1-r)\theta \right)^2}. \quad (\text{S11})$$

Using Eq. (S8), we have

$$\lambda_G = -\alpha \mathbb{E}[s_0] \frac{1 - \frac{\alpha}{\mu \mathbb{E}[s_0]^2} (1-r)\theta}{\alpha 1 + \frac{\alpha}{\mu \mathbb{E}[s_0]} (1-r)\theta} = \frac{\frac{\alpha}{\mu} (1-r)\theta}{\mathbb{E}[s_0] + \frac{\alpha}{\mu} (1-r)\theta} = \frac{\mathbb{E}[\Delta s]}{\mathbb{E}[s_f]} = \frac{1}{2}, \quad (\text{S12})$$

and

$$\text{CV}_{s_0}^2 = \frac{\alpha^2}{3} \frac{1}{\alpha^2} \frac{\left(\frac{\alpha}{\mu \mathbb{E}[s_0]} \right)^2 (1-r)\theta}{\left(1 + \frac{\alpha}{\mu \mathbb{E}[s_0]} (1-r)\theta \right)^2} \approx \frac{1}{3(1-r)\theta}. \quad (\text{S13})$$

These corresponds to the intrinsic limit solutions considered in the main text.

An alternative and equivalent formula for the division control parameter can be derived noting that the conditional expected value of the first-passage time satisfies

$$\mathbb{E}[\tau^{(i)}|s_0^{(i)}] = \mathbb{E}[\tau] + \frac{\text{Cov}[\tau^{(i)}, s_0^{(i)}]}{\text{Var}[s_0]} (s_0^{(i)} - \mathbb{E}[s_0]). \quad (\text{S14})$$

Considering exponential growth, $s_f^{(i)} = s_0^{(i)} e^{\alpha \tau^{(i)}}$, and keeping only linear-order fluctuations, one has:

$$\mathbb{E}[\tau^{(i)}|s_0^{(i)}] = \frac{1}{\alpha} \log \left(\frac{\mathbb{E}[s_f^{(i)}|s_0^{(i)}]}{s_0^{(i)}} \right), \quad (\text{S15})$$

and

$$\text{Cov}[\tau^{(i)}, s_0^{(i)}] = \frac{1}{\alpha \mathbb{E}[s_0]} \left(\frac{\text{Cov}[s_f^{(i)}, s_0^{(i)}]}{e^{\alpha \mathbb{E}[\tau]}} - \text{Var}[s_0] \right). \quad (\text{S16})$$

Inserting this expression into Eq. (S14) and using Eq. (S8) we find

$$\lambda_G = 1 - \frac{1}{2} \frac{\text{Cov}[s_f^{(i)}, s_0^{(i)}]}{\text{Var}[s_0]}. \quad (\text{S17})$$

C. EFFECTS OF THRESHOLD FLUCTUATIONS ON DIVISION CONTROL

As discussed in the main text, in the presence of threshold fluctuations

$$\theta^i = (1-\rho)\langle\theta\rangle + \rho\theta^{i-1} + \eta^i, \quad \eta^i \stackrel{\text{i.i.d.}}{\sim} \mathcal{N}(0, \sigma_{\text{extr.}}^2), \quad (\text{S18})$$

with

$$\text{Var}(\theta^i) = \sigma_\theta^2 = \sigma_{\text{extr.}}^2 / (1 - \rho^2), \quad \text{Cov}(\theta^{i-k}, \theta^i) = \rho^k \sigma_\theta^2, \quad (\text{S19})$$

Eq. (1) of the main text should be replaced with

$$s_f^i = s_0^i + \frac{\alpha}{\mu} (\theta^i - r\theta^{i-1}), \quad s_0^i = \frac{s_f^{i-1}}{2}. \quad (\text{S20})$$

We will now use Eq. (S20) to derive the expressions for size fluctuations and division control parameter reported in Eq. (5) of the main text.

Linear regression between birth and division size

We start by computing the slope of the linear regression between birth and division size, defined as $1 - \zeta_\Delta = \text{Cov}(s_f^i, s_0^i) / \sigma_{s_0}^2$.

Using Eq. (S20),

$$\text{Cov}(s_f^i, s_0^i) = \sigma_{s_0}^2 + \frac{\alpha}{\mu} [\text{Cov}(\theta^i, s_0^i) - r \text{Cov}(\theta^{i-1}, s_0^i)], \quad (\text{S21})$$

so that it remains to evaluate $\text{Cov}(\theta^i, s_0^i)$ and $\text{Cov}(\theta^{i-1}, s_0^i)$.

Calculation of $\text{Cov}(\theta^i, s_0^i)$. To compute this term, we use symmetric division, $s_0^i = s_f^{i-1} / 2$, and Eq. (S20), to write

$$\begin{aligned} \text{Cov}(\theta^i, s_0^i) &= \frac{1}{2} \text{Cov}(\theta^i, s_f^{i-1}) = \frac{1}{2} \text{Cov}\left(\theta^i, s_0^{i-1} + \frac{\alpha}{\mu} (\theta^{i-1} - r\theta^{i-2})\right) \\ &= \frac{1}{2} \text{Cov}(\theta^i, s_0^{i-1}) + \frac{1}{2} \frac{\alpha}{\mu} [\text{Cov}(\theta^i, \theta^{i-1}) - r \text{Cov}(\theta^i, \theta^{i-2})]. \end{aligned} \quad (\text{S22})$$

Now, using the threshold statistics of Eq. (S19), we obtain

$$\text{Cov}(\theta^i, s_0^i) = \frac{1}{2} \text{Cov}(\theta^i, s_0^{i-1}) + \frac{1}{2} \frac{\alpha}{\mu} (\rho - r\rho^2) \sigma_\theta^2. \quad (\text{S23})$$

Finally, using the discrete-time AR(1) threshold dynamics in Eq. (S18) and the fact that η^i is independent of s_0^{i-1} , we can write

$$\text{Cov}(\theta^i, s_0^{i-1}) = \rho \text{Cov}(\theta^{i-1}, s_0^{i-1}), \quad (\text{S24})$$

so that Eq. (S23) becomes the recursion

$$\text{Cov}(\theta^i, s_0^i) = \frac{1}{2} \rho \text{Cov}(\theta^{i-1}, s_0^{i-1}) + \frac{1}{2} \frac{\alpha}{\mu} (\rho - r\rho^2) \sigma_\theta^2. \quad (\text{S25})$$

In the stationary regime, $\text{Cov}(\theta^i, s_0^i) = \text{Cov}(\theta^{i-1}, s_0^{i-1})$, and solving Eq. (S25) yields

$$\text{Cov}(\theta^i, s_0^i) = \frac{1}{2} \frac{\alpha}{\mu} \frac{\rho - r\rho^2}{1 - \rho/2} \sigma_\theta^2. \quad (\text{S26})$$

Calculation of $\text{Cov}(\theta^{i-1}, s_0^i)$: Following similar algebraic steps, and using the AR(1) relation $\text{Cov}(\theta^{i-1}, s_0^{i-1}) = \text{Cov}(\theta^i, s_0^i)$ in stationarity, we obtain

$$\text{Cov}(\theta^{i-1}, s_0^i) = \frac{1}{2} \text{Cov}(\theta^{i-1}, s_0^{i-1}) + \frac{1}{2} \frac{\alpha}{\mu} (1 - r\rho) \sigma_\theta^2 = \frac{1}{2} \frac{\alpha}{\mu} \frac{1 - r\rho}{1 - \rho/2} \sigma_\theta^2. \quad (\text{S27})$$

Now substituting Eqs. (S26) and (S27) into Eq. (S21), we obtain

$$\text{Cov}(s_f^i, s_0^i) = \sigma_{s_0}^2 + \frac{1}{2} \left(\frac{\alpha}{\mu} \right)^2 \sigma_\theta^2 \frac{(1 - r\rho)(\rho - r)}{1 - \rho/2}. \quad (\text{S28})$$

Hence, in a stationary condition, the slope of the linear regression between birth and division size becomes

$$1 - \zeta_\Delta = 1 + \frac{1}{2} \left(\frac{\alpha}{\mu} \right)^2 \frac{\sigma_\theta^2}{\sigma_{s_0}^2} \frac{(1 - r\rho)(\rho - r)}{1 - \rho/2}. \quad (\text{S29})$$

Size fluctuations

As explained in the text, to compute $\sigma_{s_0}^2$ in the presence of threshold fluctuations, we can use the law of total variance

$$\sigma_{s_0}^2 = \langle \sigma_{s_0|\theta}^2 \rangle + \sigma_{\langle s_0|\theta \rangle}^2, \quad (\text{S30})$$

where $\sigma_{s_0|\theta}^2$ denotes the variance of s_0 conditioned on a fixed threshold, and $\sigma_{\langle s_0|\theta \rangle}^2$ is the variance of the conditional mean across threshold realizations.

Calculation of first term. The birth-size variance at a fixed threshold, coming from intrinsic molecular fluctuations, has already been calculated in [5], yielding

$$\langle \sigma_{s_0|\theta}^2 \rangle = \frac{\alpha}{\mu} \frac{\langle s_0 \rangle}{3} = \left(\frac{\alpha}{\mu} \right)^2 \frac{(1 - r) \langle \theta \rangle}{3}, \quad (\text{S31})$$

where for the last equality, we have substituted the expression $\langle s_0 \rangle = \frac{\alpha}{\mu} (1 - r) \langle \theta \rangle$.

Calculation of second term. Next, we compute $\sigma_{\langle s_0|\theta \rangle}^2 \equiv \text{Var}(\langle s_0^i | \{\theta\} \rangle)$. Using Eq. (S20) and setting $m_i \equiv \langle s_0^i | \{\theta\} \rangle$, we obtain

$$m_i = \frac{1}{2} m_{i-1} + \frac{\alpha}{2\mu} (\theta^{i-1} - r\theta^{i-2}). \quad (\text{S32})$$

Let $\sigma_m^2 \equiv \text{Var}(m_i)$ in stationarity. Taking the variance of Eq. (S32) gives

$$\sigma_m^2 = \frac{1}{3} \left(\frac{\alpha}{\mu} \right)^2 \text{Var}(\theta^{i-1} - r\theta^{i-2}) + \frac{2}{3} \frac{\alpha}{\mu} \left(\text{Cov}(m_{i-1}, \theta^{i-1}) - r \text{Cov}(m_{i-1}, \theta^{i-2}) \right). \quad (\text{S33})$$

Substituting Eqs. (S26) and (S27) into Eq. (S33) and solving for σ_m^2 yields

$$\sigma_{\langle s_0|\theta \rangle}^2 = \frac{1}{3} \left(\frac{\alpha}{\mu} \right)^2 \sigma_\theta^2 \left[(1 + r^2 - 2r\rho) + \frac{(\rho - r)(1 - r\rho)}{(1 - \rho/2)} \right]. \quad (\text{S34})$$

Putting all together, we obtain the total birth size variance as

$$\sigma_{s_0}^2 = \frac{1}{3} \left(\frac{\alpha}{\mu} \right)^2 \left((1-r) \langle \theta \rangle + \sigma_\theta^2 \left[(1+r^2-2r\rho) + \frac{(\rho-r)(1-r\rho)}{(1-\rho/2)} \right] \right). \quad (\text{S35})$$

Variance in terms of relative threshold to molecular noise. Following the main text, we introduce a dimensionless noise ratio that quantifies the relative strength of extrinsic noise from threshold fluctuations to intrinsic noise from molecular fluctuations, given as follows

$$\Sigma^2 \equiv \frac{\text{CV}_{\text{extr.}}^2}{\text{CV}_{\text{mol}}^2} = (1-\rho^2) \frac{\text{CV}_\theta^2}{\text{CV}_{\text{mol}}^2} = (1-\rho^2) \tilde{\Sigma}^2, \quad (\text{S36})$$

where $\text{CV}_\theta^2 = \sigma_\theta^2 / \langle \theta \rangle^2$ and $\text{CV}_{\text{mol}}^2 = \langle \sigma_{s_0|\theta}^2 \rangle / \langle s_0 \rangle^2 = 1 / [(1-r) \langle \theta \rangle]$. In terms of this dimensionless quantity the birth size variance can be written as:

$$\sigma_{s_0}^2 = \frac{\sigma_\theta^2}{3} \left(\frac{\alpha}{\mu} \right)^2 \left(\frac{(1-r)^2}{\tilde{\Sigma}^2} + (1+r^2-2r\rho) + \frac{(\rho-r)(1-r\rho)}{(1-\rho/2)} \right). \quad (\text{S37})$$

Dividing Eq. (S37) by $\langle s_0 \rangle^2$ we can get the expression for the coefficient of variation of birth size fluctuations as

$$\text{CV}_{s_0}^2 = \text{CV}_{\text{mol}}^2 \left[1 + \frac{(1+r^2-2r\rho)(1-\rho/2) + (\rho-r)(1-r\rho)}{(1-r)^2(1-\rho/2)} \tilde{\Sigma}^2 \right]. \quad (\text{S38})$$

One can easily check that this expression is equivalent to the one reported in the main text.

Division control parameter

To obtain the expression for the division control parameter, we can substitute Eq. (S37) into Eq. (S29) to write

$$1 - \zeta_\Delta = 1 + \frac{3}{2} \frac{(\rho-r)(1-r\rho)}{(\rho-r)(1-r\rho) + (1-\rho/2) \left[\frac{(1-r)^2}{\tilde{\Sigma}^2} + (1+r^2-2r\rho) \right]}, \quad (\text{S39})$$

from which, using Eq. (S4), we have:

$$\lambda_G = \frac{1}{2} \left(1 - \frac{3}{2} \frac{(\rho-r)(1-r\rho)}{(\rho-r)(1-r\rho) + (1-\rho/2) \left[\frac{(1-r)^2}{\tilde{\Sigma}^2} + (1+r^2-2r\rho) \right]} \right), \quad (\text{S40})$$

which is equivalent to the one reported in the main text.

D. EFFECTS OF PROTEIN RESET FRACTION FLUCTUATIONS

For simplicity, in the following analysis we assume $\rho = 0$. By following the same steps leading to Eq. (S29), one finds that, in the presence of noise in the protein reset fraction r , the expression for $1 - \zeta_\Delta$ in the case of uncorrelated thresholds remains identical to Eq. (S29) evaluated at $\rho = 0$:

$$1 - \zeta_\Delta = 1 - \frac{r}{2} \left(\frac{\alpha}{\mu} \cdot \frac{\sigma_\theta}{\sigma_{s_0}} \right)^2. \quad (\text{S41})$$

However, the expression for the variance of the birth size differs in this case. For uncorrelated thresholds, using Eq. (S20) we obtain

$$3\sigma_{\langle s_0 | \theta \rangle}^2 = \left(\frac{\alpha}{\mu} \right)^2 [\text{Var}(\theta) + \text{Var}(r\theta)] - 2\langle r \rangle \left(\frac{\alpha}{\mu} \right) \text{Cov}(s_0^i, \theta^{i-1}), \quad (\text{S42})$$

$$\sigma_{\langle s_0 | \theta \rangle}^2 = \left(\frac{\alpha}{\mu} \right)^2 \frac{\sigma_\theta^2}{3} \left[1 + \langle r \rangle^2 - \langle r \rangle + \sigma_r^2 \left(1 + \frac{\langle \theta \rangle^2}{\sigma_\theta^2} \right) \right], \quad (\text{S43})$$

where Eq. (S27) has been used for $\text{Cov}(s_0^i, \theta^{i-1})$ in the limit $\rho \rightarrow 0$. Applying the law of total variance and combining with Eq. (S31), we obtain

$$\sigma_{s_0}^2 = \left(\frac{\alpha}{\mu} \right)^2 \left[(1-r) \frac{\langle \theta \rangle}{3} + \left(1 + \langle r \rangle^2 - \langle r \rangle + \sigma_r^2 \left(1 + \frac{\langle \theta \rangle^2}{\sigma_\theta^2} \right) \right) \frac{\sigma_\theta^2}{3} \right]. \quad (\text{S44})$$

In the absence of noise in the protein reset fraction, i.e. for $\sigma_r = 0$, the expression for $\sigma_{s_0}^2$ reduces to Eq. (S35) evaluated at $\rho = 0$. In contrast, increasing noise in the protein reset fraction reduces the correction term in Eq. (S41). Therefore, while threshold noise drives the system away from the intrinsic adder behavior, fluctuations in the protein reset fraction act to restore a more adder-like behavior.

E. EFFECTS OF CONSTANT DEGRADATION OF DIVISOR PROTEIN

Including a degradation term $-\gamma x^{(i)}(t)$, in the synthesis dynamics of the divisor protein modifies Eq. (S20), introduced in Section C, which now takes the more general form

$$s_f^i = s_0^i 2^{-\epsilon} + \frac{\alpha}{\mu} (1 + \epsilon) (\theta^i - r\theta^{i-1} 2^{-\epsilon}), \quad (\text{S45})$$

where $\epsilon = \gamma/\alpha$ denotes the ratio between the degradation rate and the cellular growth rate. In the limit of $\epsilon \rightarrow 0$, the above Eq. (S45) converges to Eq. (S20). We will now use Eq. (S45) to derive the expressions for size fluctuations and division control parameter. For simplicity, we assume $\rho = 0$ in the subsequent calculations.

Linear regression between birth and division size

Following the same steps as in Section C

$$\begin{aligned}\text{Cov}(s_f^i, s_0^i) &= \text{Cov}\left(s_0^i 2^{-\epsilon} + \frac{\alpha}{\mu}(1 + \epsilon)(\theta^i - r\theta^{i-1}2^{-\epsilon}), s_0^i\right), \\ &= 2^{-\epsilon}\sigma_{s_0}^2 + \frac{\alpha}{\mu}(1 + \epsilon) [\text{Cov}(\theta^i, s_0^i) - r2^{-\epsilon}\text{Cov}(\theta^{i-1}, s_0^i)].\end{aligned}\quad (\text{S46})$$

Furthermore, $\text{Cov}(\theta^i, s_0^i) = 0$ and

$$\text{Cov}(\theta^{i-1}, s_0^i) = \frac{1}{2}\text{Cov}(\theta^{i-1}, s_f^{i-1}) = \frac{1}{2}\frac{\alpha}{\mu}(1 + \epsilon)\sigma_\theta^2,$$

so that

$$1 - \zeta_\Delta \equiv \frac{\text{Cov}(s_f, s_0)}{\sigma_{s_0}^2} = \frac{1}{2^\epsilon} \left[1 - (1 + \epsilon)^2 \frac{r}{2} \left(\frac{\alpha}{\mu}\right)^2 \frac{\sigma_\theta^2}{\sigma_{s_0}^2} \right].\quad (\text{S47})$$

From Eq. (S47), we can compute the division control parameter λ_G as

$$\lambda_G = 1 - \frac{1 - \zeta_\Delta}{2} = 1 - \frac{1}{2^{\epsilon+1}} \left[1 - (1 + \epsilon)^2 \frac{r}{2} \left(\frac{\alpha}{\mu}\right)^2 \frac{\sigma_\theta^2}{\sigma_{s_0}^2} \right].\quad (\text{S48})$$

Size fluctuations

We compute the variance of cell size at birth using the law of total variance (Eq. (S30)).

Calculation of variance for fixed threshold: The birth-size variance at a fixed threshold has already been calculated in [5], yielding

$$\langle \sigma_{s_0|\theta}^2 \rangle = \left(\frac{\alpha}{\mu}\right)^2 (1 + \epsilon)^2 \frac{(1 - r2^{-\epsilon})\langle \theta \rangle}{(4 - 2^{-2\epsilon})},\quad (\text{S49})$$

which converges to Eq. (S31) for $\epsilon \rightarrow 0$.

Calculation of variance for threshold fluctuations: To compute, $\sigma_{\langle s_0|\theta \rangle}^2 \equiv \text{Var}(\langle s_0^i | \{\theta\} \rangle)$ we use Eq. (S45) and the hypothesis of uncorrelated threshold to obtain

$$\sigma_{\langle s_0|\theta \rangle}^2 = \sigma_\theta^2 \left(\frac{\alpha}{\mu}\right)^2 (1 + \epsilon)^2 \frac{(1 - r2^{-2\epsilon} + r^2 2^{-2\epsilon})}{(4 - 2^{-2\epsilon})}.\quad (\text{S50})$$

Now using Eqs. (S49) and (S50), we obtain the total birth size variance as

$$\sigma_{s_0}^2 = \frac{(1 + \epsilon)^2}{(4 - 2^{-2\epsilon})} \left(\frac{\alpha}{\mu}\right)^2 [(1 - r2^{-\epsilon})\langle \theta \rangle + \sigma_\theta^2(1 - r2^{-2\epsilon} + r^2 2^{-2\epsilon})].\quad (\text{S51})$$

In the limit $\epsilon \rightarrow 0$, Eq. (S47) and Eq. (S51) reduce to Eq. (S29) and Eq. (S35), respectively, with $\rho \rightarrow 0$ in the case of uncorrelated thresholds. In the opposite limit, $\epsilon \gg 1$, one finds $\lambda_G \simeq 1 - \frac{1}{2^{\epsilon+1}} \left[1 - \frac{2r\sigma_\theta^2}{\langle \theta \rangle + \sigma_\theta^2} \right] \rightarrow 1$, thus driving the system toward increasingly sizer-like behavior. The $\sigma_\theta^2 \rightarrow 0$ limit, $\lambda_G \rightarrow 1 - 2^{-(\epsilon+1)}$, was also studied in [5].

F. EFFECTS OF CONSTANT PRODUCTION OF DIVISOR PROTEIN

Including a constant production term ν , in the synthesis dynamics of the divisor protein modifies Eq. (S20), introduced in Section C, which now takes the more general form

$$s_f^i = s_0^i + \frac{\alpha}{\mu} (\theta^i - r\theta^{i-1} - \nu\tau^i), \quad (\text{S52})$$

where τ^i is the division time at which $x^i(t)$ reaches the threshold level for the first time. In the limit of $\nu \rightarrow 0$, the above Eq. (S52) converges to Eq. (S20). We will now use Eq. (S52) to derive the expressions for size fluctuations and division control parameter. For simplicity, we assume $\rho = 0$ in the subsequent calculations.

Linear regression between birth and division size

Following the same steps as in Section C,

$$\begin{aligned} \text{Cov}(s_f^i, s_0^i) &= \text{Cov}\left(s_0^i + \frac{\alpha}{\mu} (\theta^i - r\theta^{i-1} - \nu\tau^i), s_0^i\right), \\ &= \sigma_{s_0}^2 + \frac{\alpha}{\mu} [\text{Cov}(\theta^i, s_0^i) - r \text{Cov}(\theta^{i-1}, s_0^i) - \nu \text{Cov}(\tau^i, s_0^i)]. \end{aligned} \quad (\text{S53})$$

Furthermore, $\text{Cov}(\theta^i, s_0^i) = 0$. By considering small noise approximation around mean value $s_0^i = \langle s_0 \rangle + \Delta_i$, the other two covariances will be given as below:

$$\text{Cov}(s_0^i, \tau^i) = \text{Cov}\left(s_0^i, \frac{1}{\alpha} \ln\left(\frac{s_f^i}{s_0^i}\right)\right) \quad (\text{S54})$$

$$= \frac{1}{\alpha} \left[\text{Cov}\left(s_0^i, \ln\left(1 + \frac{\Delta_{i+1}}{\langle s_0 \rangle}\right)\right) - \text{Cov}\left(s_0^i, \ln\left(1 + \frac{\Delta_i}{\langle s_0 \rangle}\right)\right) \right] \quad (\text{S55})$$

$$\approx \frac{1}{\alpha} \left[\text{Cov}\left(s_0^i, \frac{\Delta_{i+1}}{\langle s_0 \rangle}\right) - \text{Cov}\left(s_0^i, \frac{\Delta_i}{\langle s_0 \rangle}\right) \right] \quad (\text{S56})$$

$$\approx \frac{\sigma_{s_0}^2}{\alpha \langle s_0 \rangle} \left(\frac{1 - \zeta_\Delta}{2} - 1 \right), \quad [1 - \zeta_\Delta = \text{Cov}(s_f^i, s_0^i) / \sigma_{s_0}^2] \quad (\text{S57})$$

$$\text{Cov}(s_0^i, \theta^{i-1}) = \frac{1}{2} \text{Cov}(s_f^{i-1}, \theta^{i-1}) = \frac{1}{2} \frac{\alpha}{\mu} \text{Cov}(\theta^{i-1}, \theta^{i-1}) - \frac{\nu \alpha}{2 \mu} \text{Cov}(\tau_{i-1}, \theta^{i-1}) \quad (\text{S58})$$

$$= \frac{\alpha \sigma_\theta^2}{2\mu} - \frac{\nu \alpha}{2\mu} \text{Cov}\left(\frac{1}{\alpha} \ln\left(\frac{s_f^i}{s_0^i}\right), \theta^{i-1}\right) \quad (\text{S59})$$

$$= \frac{\alpha \sigma_\theta^2}{2\mu} - \frac{\nu}{2\mu \langle s_0 \rangle} \text{Cov}(\Delta_i, \theta^{i-1}) \quad (\text{S60})$$

$$\text{Cov}(s_0^i, \theta^{i-1}) = \frac{\alpha \sigma_\theta^2}{\mu(2 + \omega)}, \quad (\text{S61})$$

where $\omega = \nu/(\mu\langle s_0 \rangle)$. Now, substituting Eqs. (S57) and (S61) into Eq. (S53), we obtain

$$1 - \zeta_\Delta = \frac{\text{Cov}(s_f, s_0)}{\sigma_{s_0}^2} = \frac{1}{1 + \omega/2} \left(1 + \omega - \frac{r}{2 + \omega} \left(\frac{\alpha}{\mu} \right)^2 \frac{\sigma_\theta^2}{\sigma_{s_0}^2} \right). \quad (\text{S62})$$

From Eq. (S62), we can compute the division control parameter λ_G as

$$\lambda_G = 1 - \frac{1}{2 + \omega} \left(1 + \omega - \frac{r}{2 + \omega} \left(\frac{\alpha}{\mu} \right)^2 \frac{\sigma_\theta^2}{\sigma_{s_0}^2} \right). \quad (\text{S63})$$

Size fluctuations

We compute the variance of cell size at birth using the law of total variance (Eq. (S30)).

Calculation of variance for fixed threshold. The birth-size variance at a fixed threshold has already been calculated in [5], yielding

$$\langle \sigma_{s_0|\theta}^2 \rangle = \left(\frac{\alpha}{\mu} \right)^2 \left(\langle \theta \rangle (1 - r) - \omega \langle s_0 \rangle \frac{\mu}{\alpha} \ln 2 \right) \frac{1}{(3 + 2\omega)}, \quad (\text{S64})$$

which converges to Eq. (S31) for $\omega \rightarrow 0$.

Calculation of variance for threshold fluctuations. To compute $\sigma_{\langle s_0|\theta \rangle}^2 \equiv \text{Var}(\langle s_0^i | \{\theta\} \rangle)$, we use Eq. (S52) and the hypothesis of uncorrelated threshold to obtain

$$\sigma_{\langle s_0|\theta \rangle}^2 = \sigma_\theta^2 \left(\frac{\alpha}{\mu} \right)^2 \frac{1 + r^2 - \frac{2(r+\omega)}{2+\omega} + \frac{\omega(\omega+1)}{1+\omega/2} \cdot \frac{r}{2+\omega}}{3 - \frac{\omega(\omega+1)}{1+\omega/2}}. \quad (\text{S65})$$

Now using Eq. (S64) and Eq. (S65), we can write the total birth size variance as

$$\sigma_{s_0}^2 = \left(\frac{\alpha}{\mu} \right)^2 \left[\left(\langle \theta \rangle (1 - r) - \omega \langle s_0 \rangle \frac{\mu}{\alpha} \ln 2 \right) \frac{1}{(3 + 2\omega)} + \sigma_\theta^2 \frac{1 + r^2 - \frac{2(r+\omega)}{2+\omega} + \frac{\omega(\omega+1)}{1+\omega/2} \cdot \frac{r}{2+\omega}}{3 - \frac{\omega(\omega+1)}{1+\omega/2}} \right]. \quad (\text{S66})$$

In the limit of $\omega \rightarrow 0$, Eq. (S62) and Eq. (S66) converge to Eq. (S29) and Eq. (S35), respectively, with $\rho \rightarrow 0$ for uncorrelated threshold. For $\omega \gg 1$, instead, $\lambda_G \simeq \frac{1}{2+\omega} + \frac{2r \ln 2 \sigma_\theta^2}{(1-r)\langle \theta \rangle + \omega \ln 2 (1-2r-r^2)\sigma_\theta^2} \propto \frac{1}{\omega} \rightarrow 0$ at fixed σ_θ^2 , thus driving the system towards increasingly timer-like behavior. The $\sigma_\theta^2 \rightarrow 0$ limit, $\lambda_G = 1/(2 + \omega)$, was also studied in [5].

Symbol	Description
s	Cell size
x	Copy number of divisor protein
s_0^i	Birth size in cycle i
s_f^i	Division size in cycle i
r	Protein reset fraction
τ	Division time
α	Exponential growth rate
μ	Size-dependent production rate of x
ν	Constant production rate of x
γ	Degradation rate of x
θ	Threshold level
ρ	Threshold memory between cycles
η	Extrinsic threshold noise
$\sigma_{\text{extr.}}^2$	Variance of extrinsic noise
$\langle \cdot \rangle, \mathbb{E}[\cdot]$	Ensemble mean
$\sigma_{(\cdot)}^2, \text{Var}[\cdot]$	Ensemble variance
CV	Coefficient of variation
$1 - \zeta_\Delta$	Birth–division regression slope
λ_G	Division-control parameter
Σ	Relative extrinsic/molecular noise strength

TABLE S1. Symbols used throughout the manuscript.

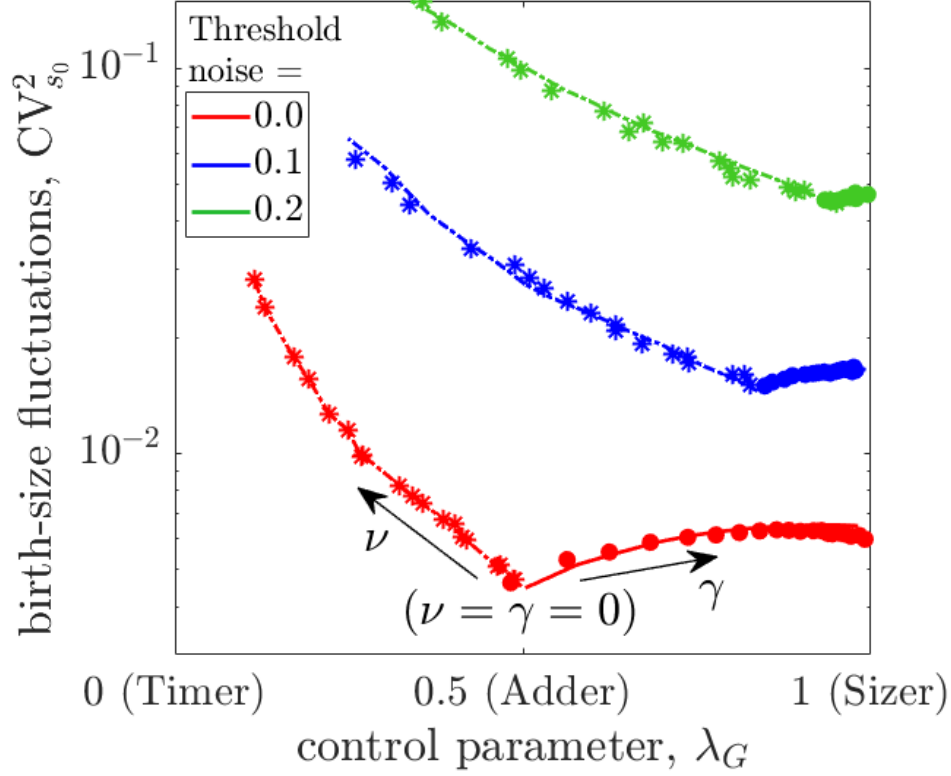


FIG. S1. **The noise in birth size is optimum when the degradation rate (γ) and the constant production rate (ν) of divisor protein are zero. The optimum value shifts from adder ($\lambda_G = 0.5$) to sizer ($\lambda_G = 1$) with threshold noise.** In the plot, the symbols are obtained from the simulation, and the curves are obtained from the analytical expressions. The parameter values are: $\langle \theta \rangle = 150$, $\mu = 1$, $\alpha = 0.01$, $r = 1/2$, $\rho = 0$. For the solid lines, $\nu = 0$ and γ increases from 0 to 0.01. We plot Eq. (S48) as x-axis and y-axis is (S51) normalized by $\langle s_0 \rangle^2$. For the dashed lines, $\gamma = 0$ and ν increases from 0 to 1, and we plot Eq. (S63) as x-axis. The y-axis is Eq. (S66) normalized by $\langle s_0 \rangle^2$. The optimum in the birth size fluctuations is obtained when $\gamma = \nu = 0$.

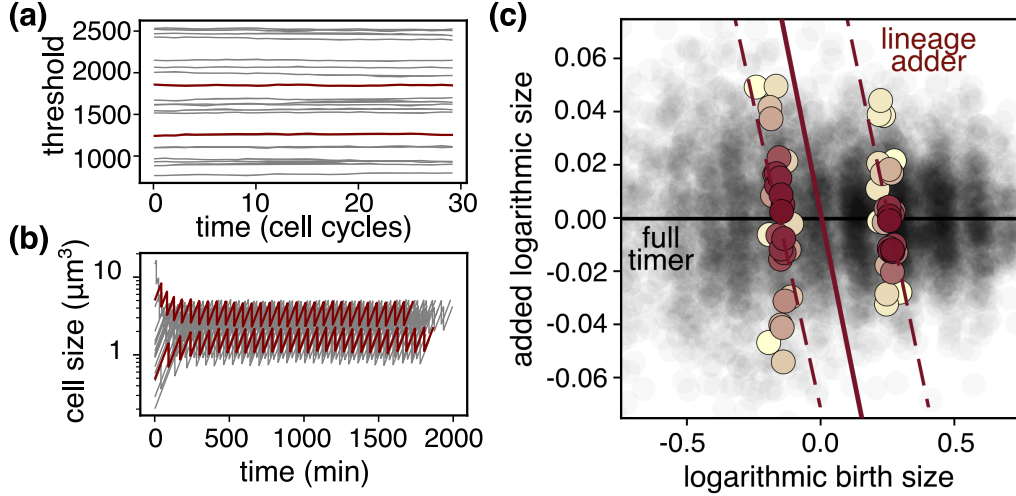


FIG. S2. **Timer control emerges from averaging lineage-specific adders in the fully autocorrelated limit.** (a)-(b) Examples of simulated threshold and cell size dynamics in the $\rho \rightarrow 1$ limit, showing stratified threshold levels arising from lineage-dependent initial conditions. (c) Size-growth plot illustrating a Simpson's paradox-like effect, where population-level timer behavior emerges from individual lineage-specific adders. Simulations with parameters: $\theta = 1000$, $\Sigma = 0.1$, $\rho = 0.99999$, $r = 0.5$, $\alpha = 0.0116 \text{ min}^{-1}$, $\mu = 5.8 \text{ min}^{-1} \mu\text{m}^{-3}$.

-
- [1] A. Amir, Cell size regulation in bacteria, *Phys. Rev. Lett.* **112** (2014).
- [2] P. Y. Ho, J. Lin, and A. Amir, Modeling cell size regulation: From single-cell-level statistics to molecular mechanisms and population-level effects, *Annu. Rev. Biophys.* **47**, 251 (2018).
- [3] J. Grilli, C. Cadart, G. Micali, M. Osella, and M. Cosentino Lagomarsino, The empirical fluctuation pattern of e. coli division control, *Front. Microbiol.* **9** (2018).
- [4] G. Micali, J. Grilli, J. Marchi, M. Osella, and M. Cosentino Lagomarsino, Dissecting the control mechanisms for DNA replication and cell division in e. coli, *Cell Rep.* **25**, 761 (2018).
- [5] M. ElGamel and A. Mugler, Effects of molecular noise on cell size control, *Phys. Rev. Lett.* **132**, 098403 (2024).
- [6] N. G. Van Kampen, *Stochastic processes in physics and chemistry*, 3rd ed., North-Holland Personal Library (North-Holland, Oxford, England, 2007).
- [7] C. Gardiner, *Stochastic Methods. A Handbook for the Natural and Social Sciences*, 5th ed., Springer Series in Synergetics (Springer Berlin Heidelberg, 2009).